2019-02-08

Autoxidation of the sea ice biomarker proxy IPSO <inf>25</inf> in the near-surface oxic layers of Arctic and Antarctic sediments

Rontani, JF

10.1016/j.orggeochem.2019.02.002
Organic Geochemistry
Elsevier BV

Autoxidation of the sea ice biomarker proxy $IPSO_{25}$ in the near-surface oxic layers of Arctic and Antarctic sediments

Jean-François Rontani[a*], Lukas Smik[b], Simon T. Belt[b]

[a] *Aix Marseille Univ, Université de Toulon, CNRS/INSU/IRD, Mediterranean Institute of Oceanography (MIO) UM 110, 13288 Marseille, France*

[b] *Biogeochemistry Research Centre, School of Geography, Earth and Environmental Sciences, University of Plymouth, Drake Circus, Plymouth, Devon PL4 8AA, UK*

* Corresponding author. Tel.: +33-4-86-09-06-02; fax: +33-4-91-82-96-41. *E-mail address*: jean-francois.rontani@mio.osupytheas.fr (J.-F. Rontani)

Abstract

Over the last decade or so, the mono- and di-unsaturated highly branched isoprenoid (HBI) lipids IP_{25} (Ice Proxy with 25 carbon atoms) and $IPSO_{25}$ (Ice Proxy for the Southern Ocean with 25 carbon atoms) have emerged as useful proxies for sea ice in the Arctic and Antarctic, respectively. A more complete understanding of their respective proxy signatures, however, requires more detailed knowledge of their stability in the water column and in sediments. In the current study, we focused on the autoxidation of $IPSO_{25}$, first by performing laboratory-based oxidation reactions on a purified sample and characterizing products based on detailed mass spectral analysis. We then analysed for the same oxidation products in near-surface sediments retrieved from the Arctic and the Antarctic, and some suspended organic matter from the Antarctic. Our data show that $IPSO_{25}$ is susceptible to partial autoxidation within the oxic layers of Arctic and Antarctic sediments, while the same processes appear not to be so important in the water column. Although the number of primary autoxidation reactions identified in sediments was not as large as in laboratory experiments, there was evidence for their subsequent modification by biotic degradation. Quantifying the extent of degradation of $IPSO_{25}$ and IP_{25} in sediments, and thus the impact of such process on the use of these biomarkers as paleo sea ice proxies, remains challenging at this stage, since most of the primary oxidation products do not accumulate, likely due to to secondary biodegradation reactions. Some interesting differences in reactivity were also observed between $IPSO_{25}$ and IP_{25} present in the same Arctic sediments. This suggests that factors other than environmental control may influence the $IPSO_{25}/IP_{25}$ ratio (i.e. DIP_{25}) in Arctic sediments.

Key words: $IPSO_{25}$; Degradation; Autoxidation; Arctic and Antarctic sediments; Biotic and abiotic interactions; IP_{25}; DIP_{25}.

1. Introduction

C_{25} and C_{30} highly branched isoprenoid (HBI) alkenes (commonly exhibiting between one and six double bonds) are ubiquitous biomarkers found in a wide range of marine and lacustrine sediments (Rowland et al., 1990; Belt et al., 2000; Sinninghe Damsté et al., 2004). Despite this, HBIs appear to be biosynthesized by a relatively small number of diatom taxa belonging to the *Haslea, Navicula, Pleurosigma, Berkeleya*, *Rhizosolenia* and *Pseudosolenia* genera (Volkman et al., 1994; Sinninghe-Damsté et al., 1999; Belt et al., 2001a, 2001b, 2016; Grossi et al., 2004; Brown et al., 2014; Kaiser et al., 2016). Amongst the more recent investigations, a mono-unsaturated C_{25} HBI alkene (3,9,13-trimethyl-6-(1,5-dimethylhexyl)-tetradec-1-ene) was identified in Arctic sea ice and in underlying sediments (Belt et al, 2007; Vare et al, 2009). Since this HBI is believed to only be made by certain Arctic sea ice diatoms (Belt et al., 2007; Brown et al., 2014) and appears relatively stable in the geological record, its analysis in marine sedimentary archives provides a proxy measure of seasonal Arctic sea ice in the past. More commonly referred to as IP_{25} (Ice Proxy with 25 carbon atoms), this HBI has been used as the basis for sea ice reconstructions spanning different Arctic regions and over a range of timescales (see Belt, 2018 for a recent compilation of sea ice reconstructions). A related di-unsaturated HBI (2,6,10,14-tetramethyl-7-(3-methylpent-4-enyl)-pentadec-6(17)-ene), sometimes referred to as diene II, is co-produced with IP_{25} in the Arctic, and is also biosynthesized by some Antarctic sea ice diatoms (Nichols et al., 1993; Johns et al., 1999; Belt et al., 2016). Interestingly, however, IP_{25} has not been reported in sea ice, sediments or the water column from around the Antarctic. As such, diene II has been proposed as a proxy measure for sea ice in the Southern Ocean, and the term $IPSO_{25}$ (Ice Proxy for the Southern Ocean with 25 carbon atoms) has been recently proposed (Belt et al., 2016). Although $IPSO_{25}$ appears to be a common

constituent of Antarctic surface sediments (for near-coastal regions, at least; Nichols et al., 1993; Johns et al., 1999; Belt et al., 2016; Belt, 2018,2019), analysis of $IPSO_{25}$ in downcore Antarctic archives has so far resulted in only a relatively small number of palaeo sea ice reconstructions, at least in comparison with IP_{25} for the Arctic (e.g., Collins et al., 2013; Etourneau et al., 2013; Barbara et al., 2016; Campagne et al., 2016; see also Belt, 2018,2019 for a recent review and summary). Finally, in the Arctic, the ratio $IPSO_{25}/IP_{25}$ (sometimes referred to as DIP_{25}) has previously been proposed as a possible indicator of variability in sea ice conditions or even of sea surface temperatures (SST) (e.g. Fahl and Stein, 2012; Stein et al., 2012; Cabedo-Sanz et al., 2013).

As with all proxies, including those based on individual or combinations of biomarkers, their application requires careful consideration of alteration and preservation between their source and sedimentary environments. It is necessary, therefore, to determine the magnitude and relative importance of various biotic and/or abiotic processes that can influence the preservation of the original source signature. In the case of HBIs, bacterial degradation of some HBIs was studied several decades ago (Robson and Rowland, 1988), yet the effects of photo- and autoxidation on these compounds have been examined only relatively recently. Motivation for the more recent studies stems partly from the proxy signatures of certain HBIs such as IP_{25} and $IPSO_{25}$, as described above, together with the now well-known high reactivity of terrestrial and marine organic matter, more generally, in the Arctic (Rontani et al., 2012,2016,2017). By studying the reactivity of a range of HBI alkenes towards different abiotic processes in solvents and in senescent diatoms (Rontani et al., 2011,2014), extremely low reactivities of mono- and di-unsaturated HBIs were observed, and attributed to the presence of relatively unreactive terminal double bonds. Such lack of reactivity is consistent with the general lack of degradation of IP_{25} in the water column following sea ice melt (Brown et al., 2016; Rontani et al., 2018a). However, lipid

autoxidation is not limited to the water column, and can potentially be an important process in the oxic layers of sediments, especially for regions of low accumulation rates, where near-surface sediments may represent relatively long time intervals (decades to centuries). Indeed, as part of a recent laboratory-based investigation into the autoxidation of IP_{25}, a series of oxidation products were characterized that could also be identified in sediment material from the Canadian Arctic (Rontani et al., 2018a). This study demonstrated the susceptibility of IP_{25} towards autoxidation in Arctic sediments, a process that was more prevalent in cases where sequestered ice algal material experienced relatively long residence times in the oxic layer. On the other hand, the near-ubiquity of IP_{25} in surface sediments from across the Arctic suggests that such oxidation reactions likely perturb its sedimentary content, rather than remove it.

In the present work, we aimed to determine whether $IPSO_{25}$ also undergoes autoxidation in near-surface Arctic and Antarctic sediments and, therefore, whether palaeo sea ice reconstructions using this proxy should consider the possible impact of this type of degradation. To achieve this, oxidation of purified $IPSO_{25}$ was carried out under more powerful oxidative conditions than previously employed (Rontani et al., 2014) and the main products were identified by high resolution mass spectral analysis. The same oxidation products were then analysed for, and quantified, in sediment samples from the Canadian Arctic and the West Antarctic Peninsula (WAP).

2. Experimental

2.1. Sediment sampling

Sediment material from the Arctic was taken from a box core obtained from Barrow Strait (STN 4) in the Canadian Arctic on board the CCGS Amundsen in 2005 (Belt et al.,

2013). The box core was sectioned on board, with sub-samples (1 cm resolution) then frozen (-20º C) prior to being freeze-dried and stored (–20º C to +4º C) prior to analysis (Rontani et al., 2018a). The redox boundary layer was identified using the change (reduction) in Mn content as described previously (Vare et al., 2009; Brown, 2011 and references cited therein). Sediment material from the WAP (see Belt et al., 2016 for details of locations) was obtained from the upper 0–1 cm of box cores collected between 2002 and 2011 and then held at the British Antarctic Survey (UK) or the British Ocean Sediment Core Research Facility (BOSCORF, UK) at +4º C. suspended particulate matter (SPM) were obtained off the coast of East Antarctica as described previously (Rontani et al., 2018b) (Supplementary Figure 1).

2.2. Chemicals

A sample of purified $IPSO_{25}$ was obtained from a culture of the marine diatom *Haslea ostrearia* as described previously (Johns et al., 1999).

Treatment of $IPSO_{25}$ with a stoichiometric amount of perchloroperbenzoic acid in dry dichloromethane (4h at 50 °C) mainly afforded 1,2-epoxy-2-(4-methylpentyl)-3-(3-methylpent-4-enyl)-6,10-dimethylundecane (**1**) (93%) (Belt et al., 2007) and to a lower extent 1,2-epoxy-3,9,13-trimethyl-6-(1-methylidene-5-methylhexyl)-tetradecane (**2**) (7%) (total yield 85%). Differentiation between these two isomers was difficult due to their very similar mass spectra and needed $LiAlH_4$-reduction to the corresponding alcohols (see below).

Oxidation of $IPSO_{25}$ using $RuCl_3$ and *tert*-butyl hydroperoxide in cyclohexane at room temperature for 16 h (Seki et al., 2008) and subsequent $NaBH_4$-reduction in ether-methanol (4:1, v/v) produced 6-methylidene-2,10,14-trimethyl-7-(3-methylpent-4-enyl)-pentadecan-5-ol (**3**) and 3,9,13-trimethyl-6-(1-methylidene-5-methylhexyl)-tetradec-1-en-

3-ol (**4**) in low yield. It is interesting to note that using a mixture of $RuCl_3$ and *tert*-butyl hydroperoxide failed to attack the tertiary allylic position at C-7, likely due to steric hindrance.

$LiAlH_4$-reduction of the mixture of epoxides **1** and **2** in dry diethyl ether (1 h at room temperature) afforded 2,6,10,14-tetramethyl-7-(3-methylpent-4-enyl)-pentadecan-6-ol (**5**) and 3,9,13-trimethyl-6-(1-methylidene-5-methylhexyl)-tetradecan-2-ol (**6**), respectively (total yield 95%).

Treatment of $IPSO_{25}$ with a stoichiometric amount of OsO_4 in dioxane-pyridine (8:1, v/v) at room temperature for 1h (MacCloskey and MacClelland, 1965) afforded 2-(4-methylpentyl)-3-(3-methylpent-4-enyl)-6,10-dimethylundecane-1,2-diol (**7**) (yield 60%).

3,9,13-trimethyl-6-(1-methylene-5-methylhexyl)-tetradecane-1,2-diol (**8**) was obtained in small amounts after hydrolysis of the epoxide **2** in a mixture of MeOH and HCl 2N (5:1, v/v) at 50 °C for 2 h. Under these conditions epoxide **1** mainly isomerized to allylic alcohols.

3,7,11,15-Tetramethylhexadecan-1,2-diol (**9**) was produced by $Pd/CaCO_3$-catalysed hydrogenation of 3-methylidene-7,11,15-trimethylhexadecan-1,2-diol (**10**) (Rontani et al., 2018), whose synthesis from phytol was described previously (Rontani and Aubert, 2005).

2,6,10,14-Tetramethylpentadecan-2-ol (**11**) was produced by condensation of 6,10,14-trimethylpentadecan-2-one (**12**) with methyllithium in anhydrous diethyl ether as previously described (Rontani et al., 2013a).

2.3. Induction of autoxidation in solvent

Autoxidation experiments were performed under an atmosphere of air in 15 ml screw-cap flasks containing $IPSO_{25}$ (10 µg), *tert*-butyl hydroperoxide (300 µl of a 6.0 M solution in decane), di-*tert*-butyl nitroxide (1.2 mg) and hexane (2 ml). After stirring, the flask was incubated in the dark at 65 °C. A relatively high temperature was selected in order to accelerate the autoxidation reactions. Aliquots (200 µl) were withdrawn from the reaction mixture after incubation for different times. Each sub-sample was evaporated to dryness under a stream of nitrogen and analyzed by gas chromatography–electron ionization quadrupole time of flight mass spectrometry (GC-QTOF) after $NaBH_4$ reduction (Section 2.5) and derivatization (Section 2.7) for identification of hydroxylated oxidation products.

2.4. Reduction of oxidation products

Hydroperoxides resulting from $IPSO_{25}$ oxidation were reduced to the corresponding alcohols by reaction with excess $NaBH_4$ in diethyl ether:methanol (4:1, v/v) at room temperature (1 h). After reduction, a saturated solution of NH_4Cl (10 ml) was added cautiously to remove any unreacted reducer; the pH was adjusted to 1 with dilute HCl (2 N) and the mixture shaken and extracted with hexane:chloroform (5 ml, 4:1, v/v; x3). The combined extracts were dried over anhydrous Na_2SO_4, filtered and evaporated to dryness under a stream of nitrogen.

2.5. Sediment and SPM treatment

Sediments or SPM material (collected on GF/F filters, porosity 0.8 µm) were placed in MeOH (15 ml) and hydroperoxides were reduced to the corresponding alcohols with excess $NaBH_4$ (70 mg, 30 min at 20 °C). Following the reduction step, water (15 ml) and KOH (1.7 g) were added and the mixture saponified by refluxing (2 h). After cooling, the contents of the flask were acidified (HCl, to pH 1) and extracted three times with

dichloromethane (DCM) (30 ml). The combined DCM extracts were dried over anhydrous Na_2SO_4, filtered and concentrated to give the total lipid extract (TLE). Since $IPSO_{25}$ oxidation product content was quite low relative to other lipids, accurate quantification required further separation of the TLE using column chromatography (silica; Kieselgel 60, 8 x 0.5 cm). $IPSO_{25}$ was recovered in the hexane eluate and its oxidation products in the dichloromethane eluate.

2.6. Derivatization

In order to analyse for hydroxylated products (i.e. alcohols and carboxylic acids), lipid extracts were derivatized by dissolving them in 300 µl pyridine/bis-(trimethylsilyl)trifluoroacetamide (BSTFA; Supelco; 2:1, v/v) and silylated (50 °C, 1 h). After evaporation to dryness under a stream of N_2, the derivatized residue was re-dissolved in 100 µl BSTFA (to avoid desilylation of fatty acids), together with an amount of solvent (ethyl acetate) dependent on the mass of the extract, and then analyzed using GC–QTOF and GC-MS/MS.

2.7. GC-QTOF analyses

Accurate mass spectra were obtained with an Agilent 7890B/7200 GC-QTOF System (Agilent Technologies, Parc Technopolis - ZA Courtaboeuf, Les Ulis, France). A cross-linked 5% phenyl-methylpolysiloxane (Macherey Nagel; Optima 5-MS Accent) column (30 m × 0.25 mm, 0.25 µm film thickness) was employed. Analysis was performed with an injector operating in pulsed splitless at 280 °C and the oven temperature programmed from 70 °C to 130 °C at 20 °C/min, then to 250 °C at 5 °C/min and then to 300 °C at 3 °C/min. The carrier gas (He) was maintained at 0.69×10^5 Pa until the end of the temperature

program. Instrument temperatures were 300 °C for transfer line and 230 °C for the ion source. Accurate mass spectra were recorded across the range *m/z* 50-700 at 4 GHz with nitrogen as collision gas (1.5 ml/min). The QTOF-MS instrument provided a typical resolution ranging from 8009 to 12252 from *m/z* 68.9955 to 501.9706. Perfluorotributylamine (PFTBA) was utilized for daily MS calibration. Structural assignments were based on interpretation of accurate mass spectral fragmentations and confirmed by comparison of retention times and mass spectra of oxidation products with those of authentic synthesized compounds.

2.8. GC-MS/MS analyses

GC/EIMS/MS experiments were performed using an Agilent 7890A/7010 tandem quadrupole gas chromatograph system equipped with a HES source (Agilent Technologies, Parc Technopolis - ZA Courtaboeuf, Les Ulis, France). A cross-linked 5% phenyl-methylpolysiloxane (Agilent; HP-5MS) (30 m × 0.25 mm, 0.25 μm film thickness) capillary column was employed. Analyses were performed with an injector operating in pulsed splitless mode set at 270 °C and the oven temperature programmed from 70 °C to 130 °C at 20 °C/min, then to 250 °C at 5 °C/min and then to 300 °C at 3 °C/min. The pressure of the carrier gas (He) was maintained at 0.69 x 10^5 Pa until the end of the temperature program and then programmed from 0.69 × 10^5 Pa to 1.49 × 10^5 Pa at 0.04 × 10^5 Pa/min. The following mass spectrometric conditions were employed: electron energy, 70 eV; transfer line, 300 °C; source temperature, 230 °C; quadrupole 1 temperature, 150 °C; quadrupole 2 temperature, 150 °C; collision gas (N_2) flow, 1.5 ml/min; quench gas (He) flow, 2.25 ml /min; mass range, 50-700 Dalton; cycle time, 313 ms. Collision induced dissociation (CID) was optimized by using collision energies at 5, 10, 15 and 20 eV. Quantification of oxidation

products **3**, **5** and **7** was carried out with external standards in multiple reaction monitoring (MRM) mode. Precursor ions were selected from the more intense and specific ions observed in EI mass spectra. Due to the very low amounts of $IPSO_{25}$ available, these compounds could not be produced in sufficient amounts to be used as external standard during their quantification in sediment samples. TMS derivative of structurally similar isoprenoid compounds (3-methylidene-7,11,15-trimethylhexadecan-1,2-diol (**10**) for compound **3**, 2,6,10,14-tetramethylpentadecan-2-ol (**11**) for compound **5** and 3,7,11,15-tetramethylhexadecan-1,2-diol (**9**) for compound **7**) (see appendix) were thus used as external standards. Correction factors that took into account the proportion of the selected precursor ion in the EIMS of each compound and that of the selected MRM transition in each CID-MS were employed.

3. Results

3.1. Autoxidation of $IPSO_{25}$ in solvent

A number of different oxidation products could be detected after incubation of $IPSO_{25}$ in hexane in the presence of *tert*-butyl hydroperoxide (radical enhancer) and di-*tert*-butyl nitroxide (radical initiator) (Porter et al., 1995) at 65 °C and subsequent $NaBH_4$-reduction and silylation. Comparison of retention times and accurate mass spectra of these compounds (Figs. 1 and 2) with qualitative standards prepared by oxidation of purified $IPSO_{25}$ (Section 2.2) allowed formal identification of compounds **1** (59.2%), **2** (5.9%), **3** (9.3%), **4** (10.2%) and **7** (traces). A compound derived from the attack of the terminal tertiary carbon atoms was also detected, and tentatively attributed to 10-methylidene-2,6,14-trimethyl-9-(3-methylpent-4-enyl)-pentadecan-2-ol (**13**) or 6-methylidene-2,10,14-

trimethyl-7-(3-methylpent-4-enyl)-pentadecan-2-ol (**14**) (7.6%) on the basis of the accurate mass fragmentations observed (Fig. 1D).

3.2. Autoxidation of IPSO$_{25}$ in Arctic and Antarctic sediments

The DCM eluates obtained after chromatographic fractionation of the total lipid extracts from the sediments investigated were analysed in MRM mode. The use of the transitions *m/z* 365 → 275, *m/z* 365 → 135 and *m/z* 365 → 149 and the comparison of retention time with the oxidation products characterized during the thermal incubation reactions allowed the unambiguous detection of the alcohol **3** (Fig. 3). In contrast, we failed to detect the oxidation products **1**, **2** and **4**. Taking into account: (i) the presence of the IPSO$_{25}$ oxidation product **3** in the sediments and (ii) the well-known lability of epoxides, we searched for the presence of the reduction and hydrolysis products of the main oxidation product **1** (i.e. 2,6,10,14-tetramethyl-7-(3-methylpent-4-enyl)-pentadecan-6-ol (**5**) (Fig. 2A) and 2-(4-methylpentyl)-3-(3-methylpent-4-enyl)-6,10-dimethylundecane-1,2-diol (**7**) (Fig. 2C)). By using appropriate MRM transitions, we were able to detect the tertiary alcohol **5** in DCM eluates of both Arctic and Antarctic sediments (Fig. 4). In contrast, diol **7** could only be identified in the Arctic sediment extracts (Fig. 5).

As described in Section 2.8, quantification of compounds **3**, **5** and **7** involved the use of TMS derivatives of structurally similar isoprenoid compounds as external standards. The transitions employed for quantification were (i) *m/z* 365 → 275 and *m/z* 353 → 263 (loss of trimethylsilanol by the precursor ion) for the alcohol **3** and the standard **10**, respectively; (ii) *m/z* 353 → 117 and *m/z* 341 → 117 (formation of the product ion TMS-O$^+$=CH-CH$_3$) for the tertiary alcohol **5** and the standard **11**, respectively; (iii) *m/z* 423 → 333 and *m/z* 355 → 265 (loss of trimethylsilanol by the precursor ion) for the diol **7** and the standard **9**, respectively.

As indicated in Section 2.8, corrective factors were applied to accommodate for structural differences between the oxidation product and the corresponding standard. The resulting concentrations of compounds **3**, **5** and **7** are given in Tables 1 and 2.

3.3. Autoxidation of IPSO$_{25}$ in Antarctic SPM

We also analysed for IPSO$_{25}$ oxidation products in lipid extracts of suspended particles collected at different water depths in the polynya region west of the Dalton Iceberg Tongue (East Antarctica) and where an intense autoxidation of some other lipids was previously observed (Rontani et al., 2018b). However, compounds **3**, **5** and **7** could not be identified in any of the samples analysed.

4. Discussion

4.1. Autoxidation of IPSO$_{25}$ in solvent

It is well-known that addition of ROO• radicals to a C=C bond competes with allylic hydrogen abstraction when there is a double bond that is either conjugated or 1,1-disubstituted (Schaich, 2005). Consistent with this, we observed efficient addition of peroxyl radicals to the 1,1-disubstituted 6-17 double bond of IPSO$_{25}$ affording epoxide **1** as the major product (59.2% of total oxidation products) after fast intramolecular homolytic substitution (Fossey et al., 1995) (Fig. 6). In contrast, addition to the terminal 23-24 double bond was relatively minor (5.9% of total oxidation products). Addition of peroxyl radicals to the 6-17 double bond also resulted in the formation of trace amounts of the diol **7** after subsequent oxygen addition and hydrogen abstraction (Fig. 6). Parallel to these peroxyl radical addition

313 reactions was a series of competitive hydrogen abstraction reactions leading to the formation
314 of hydroperoxides **15-18** (see appendix), which manifest as alcohols **3**, **4**, **13** and **14**
315 following $NaBH_4$-reduction during treatment. Hydrogen atom abstraction from the allylic
316 carbon atoms 5 and 22 of $IPSO_{25}$ and subsequent oxidation of the resulting radicals to yield
317 hydroperoxides **15** and **16**, respectively (Fig. 6), is as expected given the relatively stable
318 allylic radicals formed (Fig. 6), with the additional formation of hydroperoxides **17** and **18**
319 presumably attributable to the stability of their respective tertiary radical precursors.
320 Surprisingly, we failed to detect oxidation products resulting from hydrogen atom
321 abstraction at carbon 7, despite the stability of the tertiary allylic radical formed. These
322 results are consistent with the very low efficiency of autoxidative processes at the allylic C-
323 7 previously observed in the case of (6-17, 9-10, 23-24) HBI triene (Rontani et al., 2014).
324 We suggest that the lack of reaction at C-7 results from steric hindrance during hydrogen
325 abstraction by the bulky *tert*-butylperoxyl radicals employed during the incubation, and is
326 supported by the lack of oxidation of the allylic carbon 7 observed during treatment of
327 $IPSO_{25}$ with $RuCl_3$- *tert*-butyl hydroperoxide (see Section 2.2). Hydrogen atom abstraction
328 from non-allylic tertiary carbon atoms appeared to be limited to the external tertiary carbon
329 atoms 2 and 14 of the molecule (and not to carbon 10), also likely due to steric hindrance.

330

331 *4.2. Degradation of $IPSO_{25}$ in Arctic and Antarctic sediments*

332 Despite the relative recalcitrance of mono- and di-unsaturated HBIs towards free
333 radical oxidation, reported previously (Rontani et al., 2011, 2014), oxidation product **3** could
334 be detected in most of the Arctic and Antarctic sediments (Tables 1 and 2), confirming the
335 partial autoxidation of $IPSO_{25}$ in both regions. On the other hand, the failure to detect the
336 major oxidation product of this diene in the incubation experiments (i.e. compound **1**) likely
337 results from: (i) the lack of specificity of its main MRM transitions, thus making it difficult

to identify, (ii) an intense degradation during the treatment ($NaBH_4$-reduction, alkaline hydrolysis and acidification) or (iii) the well-known biotic and abiotic lability of epoxides in sediments, more generally. Indeed, epoxides may undergo alcoholysis and hydrolysis during alkaline hydrolysis and are converted to chlorohydrins during acidification with HCl (Marchand and Rontani, 2001). Some epoxides are also slowly reduced to alcohols during $NaBH_4$-reduction (Zabeti et al., 2010), but this is not the case for epoxide **1**. From a biological perspective, these epoxides react readily with a large number of cell components such as DNA or proteins (Swaving and de Bont, 1998) so their removal is essential for bacteria to survive. This involves two main types of enzymes: glutathione transferases (GSTs) (which catalyse the reduction of the epoxide ring to an alcohol, Kieslich et al., 1986) and epoxide hydrolases (which catalyse the hydrolysis of the epoxide ring to a diol, Michaels et al., 1980; Rustemov et al., 1991). Moreover, epoxides may also be hydrolysed abiotically (Minerath et al., 2009) and rearranged to carbonyl compounds in sediments with high clay content (Ruiz-Hitzky and Casal, 1985).

The presence of the tertiary alcohol **5** in the sediments investigated (Tables 1 and 2), may therefore potentially be attributed to the reduction of the epoxide ring of the $IPSO_{25}$ oxidation product **1** by sedimentary bacteria (Fig. 7). However, alcohol **5** might also be produced directly from $IPSO_{25}$ by bacteria after hydration (pathway II in Fig. 7) or epoxidation (pathway III in Fig. 7) and subsequent reduction (pathway IV in Fig. 7). Indeed, the involvement of hydration during anaerobic bacterial degradation of isoprenoid alkenes (squalene, pristenes and phytenes, Rontani et al., 2002, 2013a) and *n*-alk-1-enes (Grossi et al., 2011) was demonstrated previously. On the other hand, bacterial epoxidation (mediated by cytochrome P-450-dependent monooxygenases) can produce epoxides from a broad range of lipophilic substrates such as *n*-alkenes (Soltani et al., 2004), terpenes (Duetz et al., 2003), unsaturated fatty acids (for a review see Ratledge, 1994) and alkenones (Zabeti et al.,

2010). Since bacterial epoxidation should act more intensively on the terminal 23-24 double bond due to the better proximity of the terminal double bond to the heme iron of cytochrome P-450 (Andersen et al., 1997), the formation of epoxide **2** (Fig. 7) and its degradation products would thus be expected. However, the absence of alcohol **6** (resulting from the reduction of epoxide **2** or hydration of the 23-24 double bond of $IPSO_{25}$ (Fig. 7)) in the sediments analyzed points to the lack of such bacterial processes, so the formation of alcohol **5** seems thus to mainly result from bacterial reduction of the epoxide ring of autoxidation product **1**.

Further, due to the probable low reactivity of monoxygenases towards the 6-17 double bond of $IPSO_{25}$, the formation of diol **7** may be attributed to the biotic (induced by epoxide hydrolases) or abiotic (clay-catalyzed) hydrolysis of epoxide **1** (pathways V and VI in Fig. 7). The lack of methoxyhydrins and chlorohydrins derived from the degradation of the epoxide **1** in the presence of methanol and hydrochloric acid, respectively, also allow us to exclude the possible production of diol **7** during sample treatment (alkaline hydrolysis and acidification).

Surprisingly, diol **8** could not be detected during MRM analyses of the sediment extracts, despite the previous detection of its close structural analog (i.e. diol **19**) as an oxidation product of IP_{25} in the same (STN 4) sediments (Rontani et al., 2018a). We attribute this to (i) the possible coelution of diols **7** and **8** and (ii) the very weak abundance of the precursor ion at *m/z* 423 in the mass spectrum of its TMS derivative (Fig. 2D), rather than from a lack of microbial degradation of $IPSO_{25}$.

In the sediments from the Arctic (STN 4), we also note the generally increasing proportion of $IPSO_{25}$ oxidation products with depth below the redox boundary (Fig. 8), indicative of a progressive reduction of hydroperoxide **15** (produced in the oxic layer) to the corresponding alcohol **3**, together with reduction and hydrolysis of the epoxide **1** to yield

alcohol **5** and diol **7**. However, due to the proposed action of sedimentary bacteria on the autoxidation products of $IPSO_{25}$ (see earlier), the very low amounts of compounds **3**, **5** and **7** relative to their parent compound (< 1%; Fig. 8) likely underestimates the extent of abiotic degradation of $IPSO_{25}$, more generally.

In the Antarctic surface sediments, the proportion of oxidation products was always low, ranging from 0.02 to 1.1% of the residual $IPSO_{25}$ (Table 1). These differences may potentially be attributed to: (i) the ability for sedimentary bacterial communities to degrade the primary $IPSO_{25}$ autoxidation products, as described above, or (ii) the different residence times of algal material within the oxic layer of sediments, which may vary considerably according to location. On the other hand, the variable degradation extent may reflect the different times that the sediments have been kept in storage following collection; however, for the samples analyzed, the lowest percentages of degradation products were observed in the oldest samples (i.e. in BC 313/316 collected in 2002 compared to the other box cores collected in 2008 and 2011; Table 1). These results, and those obtained previously for IP_{25} (Rontani et al., 2018a), highlight the importance of the measurement of redox boundary layers in upper sections of sediment cores and sedimentation rates to estimate the residence time of algal material in the oxic environment and thus the extent of autoxidative degradation and its impact on paleo sea ice reconstruction based on the use of HBI tracers.

4.3. Degradation of $IPSO_{25}$ in Antarctic SPM

The failure to detect compounds **3**, **5** and **7** in lipid extracts of strongly autoxidized suspended particles (Rontani et al., 2018b) collected at different water depths in the polynya region west of the Dalton Iceberg Tongue (East Antarctica) is in good agreement with: (i) the relative recalcitrance of di-unsaturated HBIs towards free radical oxidation processes

(Rontani et al., 2011, 2014), and (ii) the expected short residence time of highly aggregated ice algae (i.e. the source of $IPSO_{25}$) (Riebesell, 1991; Alldredge et al., 1993; Passow, 2002) within the water column. It also enables us to exclude the possible biological formation of these compounds in ice algae.

4.4. Potential effects of degradation processes on the DIP_{25} index

Due to the co-occurrence of $IPSO_{25}$ (generally reported as diene II in the Arctic) and IP_{25} in Arctic sea ice, particles and sediments under sea ice (Belt et al., 2007; Vare et al., 2009), it has been suggested that the ratio between these two biomarkers (viz. $IPSO_{25}/IP_{25}$ or DIP_{25} (Cabedo-Sanz et al., 2013)) may potentially provide further insights into Arctic sea ice conditions (e.g. Fahl and Stein, 2012; Stein et al., 2012; Cabedo-Sanz et al., 2013). It has also been suggested that variable DIP_{25} might be indicative of changes to SST based on some empirical observations and alignment with other SST proxies (Vare et al., 2009; Cabedo-Sanz et al., 2013; Xiao et al., 2013; Müller and Stein, 2014; Ruan et al., 2017); however, there are as yet no in situ data to support these interpretations (Belt, 2018). In general, proxies based on ratios of biomarkers are better at accommodating the effects of degradative processes, even if such effects cannot be totally eliminated. Indeed, it was previously demonstrated that, under some conditions, autoxidative and biodegradation processes may act selectively on $C_{37:2}$ and $C_{37:3}$ alkenones, thus negatively impacting on the $U^{K'}_{37}$ index (for a review, see Rontani et al., 2013b). It is feasible, therefore, that differential degradation of IP_{25} and $IPSO_{25}$ may also influence the DIP_{25} ratio, with substantially increased values, as seen in some sedimentary records (Fahl and Stein, 2012; Müller and Stein, 2014) resulting from a preferential degradation of IP_{25}. Previously, however, autoxidative degradation of these two HBIs measured in solvents (Rontani et al., 2014), showed a higher degradation

rate for $IPSO_{25}$ ($k = 0.004\ h^{-1}$) compared to IP_{25} ($k = 0.001\ h^{-1}$). Unfortunately, due to the mineralisation of the major part of substrates by bacteria, comparison of the efficiency of bacterial degradation processes on IP_{25} and $IPSO_{25}$ on the basis of the quantities of metabolites detected is difficult. However, we note that significant proportions (up to 35% of the residual substrate) of 2,8,12-trimethyl-5-(1,5-dimethylhexyl)-tridecanoic acid (**20**), resulting from bacterial cleavage of the 23-24 double bond of IP_{25}, were detected in sediments from Barrow Strait (i.e. STN 4) (Rontani et al., 2018c), while we failed to detect the corresponding metabolite of $IPSO_{25}$ (i.e. 2,8,12-trimethyl-5-(1-methylidene-5-methylhexyl)-tridecanoic acid (**21**)) in the same sediments. This suggests a preferential bacterial degradation of IP_{25}, which could potentially be attributed to the presence of toxic autoxidative epoxides in algal material containing $IPSO_{25}$, which are in lower abundance (or absent) in the case of IP_{25}. More detailed analyses of factors that control the DIP_{25} ratio, however, will be required in the future.

4.5. Consequences for IP_{25}, $IPSO_{25}$ and DIP_{25}-based sea ice reconstructions

As with all lipid-based proxies, those involving HBIs such as IP_{25} and $IPSO_{25}$ require careful consideration of their alteration and preservation during transport through the water column and deposition in sediments, including determining the magnitude and relative importance of biotic and/or abiotic processes. While both autoxidative and bacterial degradation products of IP_{25} were identified and quantified previously in Arctic surficial sediments (Rontani et al., 2018c), here we demonstrated that $IPSO_{25}$ may also be affected by such processes in Arctic and Antarctic sediments. At this stage, the characterisation of signature degradation products from these biotic and abiotic processes mainly provides useful 'qualitative' indicators of diagenetic alteration of these two paleo sea ice tracers. Unfortunately, subsequent reaction of most of the primary oxidation products by

sedimentary bacteria limits their accumulation in sediments, thereby preventing any accurate quantitative estimates of the extent of degradation of IP_{25} and $IPSO_{25}$, and thus of the ratio between them (i.e. DIP_{25}). The impacts of sedimentary degradation of IP_{25} and $IPSO_{25}$ on their use as paleo sea ice proxies therefore remains difficult to assess at this stage. On the other hand, the somewhat higher accumulation of 2,8,12-trimethyl-5-(1,5-dimethylhexyl)-tridecanoic acid (**20**) in some oxic sediments could potentially provide semi-quantitative estimates of the role of bacterial degradation of IP_{25} (Rontani et al., 2018c).

5. Conclusions

The detection of reduced or hydrolyzed autoxidation products of $IPSO_{25}$ in Arctic and Antarctic sediments demonstrated that this proxy may be partially degraded abiotically in near-surface oxic sediments, especially in the case of sediment cores containing relatively thick oxic layers representing long times of deposition. Unfortunately, due to its high biotic and abiotic lability, the major autoxidation product formed (epoxide **1**) does not accumulate in sediments. In contrast, $IPSO_{25}$ appeared to be essentially unaffected by autoxidation processes in the water column.

The results obtained during this work also confirmed that, in the environment, biotic and abiotic degradation processes cannot be considered separately. Indeed, their interactions, although complex, need to be taken into account in any organic geochemical assessment.

Autoxidation reactions of HBIs appear to occur primarily at the unsaturated or allylic carbon atoms within the lipid framework. However, the production of compounds such as **13** or **14** observed during $IPSO_{25}$ autoxidation, and the previous detection of degradation products of IP_{25} in Arctic sediments resulting from the free radical oxidation of its saturated

tertiary carbon atoms (Rontani et al., 2018a), clearly show that autoxidation processes can also affect saturated compounds when algal or bacterial material experiences long residence times in the oxic layer of sediments.

Acknowledgements

Financial support from the Centre National de la Recherche Scientifique (CNRS) and the Aix-Marseille University is gratefully acknowledged. Thanks are due to the FEDER OCEANOMED (N° 1166-39417) for the funding of the apparatus employed. LS and STB are grateful to the University of Plymouth for financial support. We thank Leanne Armand and Amy Leventer for providing the SPM samples. Thanks are due to two anonymous reviewers and to the associated editor for their useful and constructive comments.

References

Alldredge, A.L., Passow, U., Logan, B.E., 1993. The abundance and significance of a class of large, transparent organic particles in the ocean. Deep-Sea Research Part I-Oceanographic Research Papers 40, 1131–1140.

Andersen, J.F., Walding, J.K., Evans, P.H., Bowers, W.S., Feyereisen, R., 1997. Substrate specificity for the epoxidation of terpenoids and active site topology of house fly cytochrome P450 6A1. Chemical Research in Toxicology 10, 156–164.

Barbara, L., Crosta, X., Leventer, A., Schmidt, S., Etourneau, J., Domack, E., Massé, G., 2016. Environmental responses of the Northeast Antarctic Peninsula to the Holocene climate variability, Paleoceanography, 31, 131–147.

508 Belt, S.T., Allard, W.G., Massé, G., Robert, J.-M., Rowland, S.J., 2000. Highly branched
509 isoprenoids (HBIs): identification of the most common and abundant sedimentary
510 isomers. Geochimica et Cosmochimica Acta 64, 3839–3851.

511 Belt, S.T., Massé, G., Allard, W.G., Robert, J.-M., Rowland, S.J., 2001a. Identification of a
512 C_{25} highly branched isoprenoid triene in the freshwater diatom *Navicula sclesvicensis*.
513 Organic Geochemistry 32, 1169–1172.

514 Belt, S.T., Massé, G., Allard, W.G., Robert, J.-M., Rowland, S.J., 2001b. C_{25} highly
515 branched isoprenoid alkenes in planktonic diatoms of the *Pleurosigma* genus. Organic
516 Geochemistry 32, 1271–1275.

517 Belt, S.T., Massé, G., Rowland, S.J., Poulin, M., Michel, C., LeBlanc, B., 2007. A novel
518 chemical fossil of palaeo sea ice: IP_{25}. Organic Geochemistry 38, 16–27.

519 Belt, S.T., Smik, L., Brown, T.A., Kim, J.H., Rowland, S.J., Allen, C.S., Gal, J.K., Shin,
520 K.H., Lee, J.I., Taylor, K.W.R., 2016. Source identification and distribution reveals the
521 potential of the geochemical Antarctic sea ice proxy $IPSO_{25}$. Nature Communications
522 7, 12655.

523 Belt, S.T., 2018. Source-specific biomarkers as proxies for Arctic and Antarctic sea ice.
524 Organic Geochemistry 125, 277–298.

525 Belt, S.T., 2019. What do IP_{25} and related biomarkers really reveal about sea ice change?
526 Quaternary Science Reviews 204, 216–219.

527 Brown, T.A., Belt, S.T., Cabedo-Sanz, P., 2014. Identification of a novel diunsaturated C_{25}
528 highly branched isoprenoid in the marine tube-dwelling diatom *Berkeleya rutilans*.
529 Environmental Chemistry Letters 12, 455–460.

Cabedo-Sanz, P., Belt, S.T., Knies, J., Husum, K., 2013. Identification of contrasting seasonal sea ice conditions during the Younger Dryas. Quaternary Science Reviews 79, 74–86.

Campagne, P., Crosta, X., Schmidt, S., Houssais, M.N., Ther, O., Massé, G., 2016. Sedimentary response to sea ice and atmospheric variability over the instrumental period off Adélie Land, East Antarctica. Biogeosciences 13, 4205–4218.

Collins, L.G., Allen, C.S., Pike, J., Hodgson, D.A., Weckström, K., Massé, G., 2013. Evaluating highly branched isoprenoids (HBIs) as an Antarctic sea-ice proxy in deep-water glacial sediments. Quaternary Science Reviews 79, 87–98.Duez, W.A., Bouwmeester, H., Beilen, J.B., Witholt, B., 2003. Biotransformation of limonene by bacteria, fungi, yeasts and plants. Applied Microbiology and Biotechnology 61, 299–301.

Etourneau, J., Collins, L.G., Willmott, V., Kim, J.H., Barbara, L., Leventer, A., Schouten, S., Sinninghe Damsté, J.S., Bianchini, A., Klein, V., Crosta, X., Massé, G., 2013. Holocene climate variations in the western Antarctic Peninsula: evidence for sea ice extent predominantly controlled by changes in insolation and ENSO variability. Climate of the Past 9, 1431–1446.

Fahl, K., Stein, R., 2012. Modern seasonal variability and deglacial/Holocene change of central Arctic Ocean sea-ice cover: New insights from biomarker proxy records. Earth and Planetary Science Letters 351–352, 123–133.

Fossey, J., Lefort, D., Sorba, J., 1995. Free Radicals in Organic Chemistry. Masson, Paris.

Grossi, V., Beker, B., Geenevasen, J.A.J., Schouten, S., Raphel, D., Fontaine, M.-F., Sinninghe Damsté, J.S., 2004. C_{25} highly branched isoprenoid alkenes from the marine benthic diatom *Pleurosigma strigosum*. Phytochemistry 65, 3049–3055.

554 Grossi, V., Cravo-Lauro, C., Rontani, J.-F., Cros, M., Hirschler-Réa, A., 2011. Anaerobic
555 oxidation of *n*-alkenes by sulphate-reducing bacteria from the genus *Desulfatiferula*: *n*-
556 ketones as potential metabolites. Research in Microbiology 162, 915–922.
557 Johns, L., Wraige, E.J., Belt, S.T., Lewis, C.A., Massé, G., Robert, J.M., Rowland, S.J.,
558 1999. Identification of a C_{25} highly branched isoprenoid (HBI) diene in Antarctic
559 sediments, Antarctic sea-ice diatoms and cultured diatoms. Organic Geochemistry 30,
560 1471–1475.
561 Kaiser, J., Belt, S.T., Tomczak, T., Brown, T.A., Wasmund, N., Arz, H.W., 2016. C_{25} highly
562 branched isoprenoid alkenes in the Baltic Sea produced by the marine planktonic diatom
563 *Pseudosolenia calcar-avis*. Organic Geochemistry 93, 51–58.
564 Kieslich, K. Abraham, W.R., Stumpf, B., Thede, B., Washausen, P., 1986. Transformation
565 of terpenoids. In: Brunke, E.J. (Ed.), Progress in Essential Oil Research. Walter de
566 Gruyter & Co., Berlin, pp. 368–394.
567 McCloskey, J.A., McClelland, M.J., 1965. Mass spectra of O-isopropylidene derivatives of
568 unsaturated fatty esters, Journal of the American Chemical Society 87, 5090–5093.
569 Marchand, D., Rontani, J.-F., 2001. Characterisation of photooxidation and autoxidation
570 products of phytoplanktonic monounsaturated fatty acids in marine particulate matter
571 and recent sediments. Organic Geochemistry 32, 287–304.
572 Michaels, B.C., Ruettinger, R.T., Fulco, A.J., 1980. Hydration of 9,10-epoxypalmitic acid
573 by a soluble enzyme from *Bacillus megaterium*. Biochemical and Biophysical Research
574 Communications 92, 1189–1195.
575 Minerath, E.C., Schultz, M.P., Elrod, M.J., 2009. Kinetics of the reactions of isoprene-
576 derived epoxides in model tropospheric aerosol solutions. Environmental Science
577 Technology 43, 8133–8139.

578 Müller, J., Stein, R., 2014. High-resolution record of late glacial sea ice changes in Fram
579 Strait corroborates ice-ocean interactions during abrupt climate shifts. Earth and
580 Planetary Science Letters 403, 446–455.
581 Nichols, D.S., Nichols, P.D., Sullivan, C.W., 1993. Fatty acid, sterol and hydrocarbon
582 composition of Antarctic sea ice diatom communities during the spring bloom in
583 McMurdo Sound. Antarctic Science 5, 271–278.
584 Passow, U., 2002. Transparent exopolymer particles (TEP) in aquatic environments.
585 Progress in Oceanography 55, 287–333.
586 Porter, N.A., Caldwell, S.E., Mills, K.A., 1995. Mechanisms of free radical oxidation of
587 unsaturated lipids. Lipids 30, 277–290.
588 Ratledge, C., 1994. Biodegradation of oils, fats and fatty acids, In: Ratledge, C. (Ed.),
589 Biochemistry of Microbial Degradation. Kluwer Academic Publishers, Dordrecht, pp.
590 89–142.
591 Riebesell U., Schloss I., Smetacek V., 1991. Aggregation of algae released from melting sea
592 ice-implications for seeding and sedimentation. Polar Biology 11, 239–248.
593 Robson, J.N., Rowland, S.J., 1988. Biodegradation of highly branched isoprenoid
594 hydrocarbons: a possible explanation of sedimentary abundance. Organic Geochemistry
595 13, 691–695.
596 Rontani, J.-F., Mouzdahir, A., Michotey, V., Bonin P., 2002. Aerobic and anaerobic
597 metabolism of squalene by a new denitrifying *Marinobacter* sp. isolated from marine
598 sediment. Archives of Microbiology 178, 279–287.
599 Rontani, J.-F., Aubert, C., 2005. Characterization of isomeric allylic diols resulting from
600 chlorophyll phytyl side chain photo- and autoxidation by electron ionization gas
601 chromatography/mass spectrometry. Rapid Communications in Mass Spectrometry 19,
602 637–646.

603 Rontani, J.-F., Belt, S.T., Vaultier, F., Brown, T.A., 2011. Visible light-induced photo-
604 oxidation of highly branched isoprenoid (HBI) alkenes: a significant dependence on the
605 number and nature of the double bonds. Organic Geochemistry 42, 812–822.
606 Rontani, J.-F., Charriere, B., Forest, A., Heussner, S., Vaultier, F., Petit, M., Delsaut, N.,
607 Fortier, L., Sempéré, R., 2012. Intense photooxidative degradation of planktonic and
608 bacterial lipids in sinking particles collected with sediment traps across the Canadian
609 Beaufort Shelf (Arctic Ocean). Biogeosciences 9, 4787–4802.
610 Rontani, J.-F., Bonin, P., Vaultier, F., Guasco, S., Volkman, J.K., 2013a. Anaerobic bacterial
611 degradation of pristenes and phytenes in marine sediments does not lead to pristane and
612 phytane. Organic Geochemistry 58, 43–55.
613 Rontani, J.-F., Volkman, J.K., Prahl, F.G., Wakeham, S.G., 2013b. Biotic and abiotic
614 degradation of alkenones and implications for $U_{37}^{K'}$ paleoproxy applications: A review.
615 Organic Geochemistry 59, 93–113.
616 Rontani, J.-F., Belt, S., Vaultier, F., Brown, T., Massé, G., 2014. Autoxidative and
617 photooxidative reactivity of highly branched isoprenoid (HBI) alkenes. Lipids, 49(5),
618 481–494.
619 Rontani, J.-F., Belt, S.T., Brown, T.A., Amiraux, R., Gosselin, M., Vaultier, F., Mundy, C.J.,
620 2016. Monitoring abiotic degradation in sinking versus suspended Arctic sea ice algae
621 during a spring ice melt using specific lipid oxidation tracers. Organic Geochemistry
622 98, 82–97.
623 Rontani, J.-F., Galeron, M.-A., Amiraux, R., Artigue, L., Belt, S.T., 2017. Identification of
624 di- and triterpenoid lipid tracers confirms the significant role of autoxidation in the
625 degradation of terrestrial vascular plant material in the Canadian Arctic. Organic
626 Geochemistry 108, 43–50.

627 Rontani, J.-F., Belt, S.T., Amiraux R., 2018a. Biotic and abiotic degradation of the sea ice
628 diatom biomarker IP_{25} and selected algal sterols in near-surface Arctic sediments.
629 Organic Geochemistry 118, 73–88.
630 Rontani, J.-F., Smik, L., Belt, S.T., Vaultier, F., Armbrecht, L., Leventer, A., Armand L.K.,
631 2018b. Abiotic degradation of highly branched isoprenoid alkenes and other lipids in
632 the water column off East Antarctica. Marine Chemistry (Submitted).
633 Rontani, J.-F., Aubert, C., Belt S.T., 2018c. EIMS Fragmentation and MRM quantification
634 of bacterial metabolites of the sea ice biomarker proxy IP_{25} in Arctic sediments. Rapid
635 Communications in Mass Spectrometry 32(10), 775–783.
636 Rowland, S.J., Hird, S.J., Robson, J.N., Venkatesan, M.I., 1990. Hydrogenation behaviour
637 of two highly branched C_{25} dienes from Antarctic marine sediments. Organic
638 Geochemistry 15, 215–218.
639 Ruan, J., Huang, Y., Shi, X., Liu, Y., Xiao, W., Xu, Y., 2017. Holocene variability in sea
640 surface temperature and sea ice extent in the northern Bering Sea: A multiple biomarker
641 study. Organic Geochemistry 113, 1–9.
642 Ruiz-Hitzky, E., Casal, B., 1985. Epoxide rearrangements on mineral and silica-alumina
643 surfaces. Journal of Catalysis 92, 291–295.
644 Rustemov, S.A., Golovieva, L.A., Alieva, R.M., Baskunov, B.P., 1991. New pathway of
645 styrene oxidation by a *Pseudomonas putida* culture. Mikrobiologiya 61, 5–10.
646 Schaich, K.M., 2005. Lipid Oxidation: Theoretical Aspects. In: Shahidi, F. (Ed.), Bailey’s
647 Industrial Oil and Fat Products. John Wiley & Sons, Chichester, pp. 269–355.
648 Seki, H., Ohyama, K., Sawai, S., Mizutani, M., Ohnishi, T., Sudo, H., Akashi, T., Aoki, T.,
649 Saito, K., Muranaka, T., 2008. Licorice β-amyrin 11-oxidase, a cytochrome P450 with
650 a key role in the biosynthesis of the triterpene sweetener glycyrrhizin. Proceedings of
651 the National Academy of Science of U.S.A. 105, 14204–14209.

652 Sinninghe Damsté, J.S., Schouten, S., Rijpstra, W.I.C., Hopmans, E.C., Peletier, H., Gieskes,
653 W.W.C., Geenevasen, J.A.J., 1999. Structural identi!cation of the C_{25} highly branched
654 isoprenoid pentaene in the marine diatom *Rhizosolenia setigera*. Organic Geochemistry
655 30, 1581–1583.
656 Sinninghe Damsté, J.S., Muyzer, G., Abbas, B., Rampen, S.W., Massé, G., Allard, W.G.,
657 Belt, S.T., Robert, J.-M., Rowland, S.J., Moldowan, J.M., Barbanti, S.M., Fago, F.J.,
658 Denisevich, P., Dahl, J., Trinidade, L.A.F., Schouten, S., 2004. The rise of the
659 rhizosolenid diatoms. Science 304, 584–587.
660 Soltani, M., Metzger, P., Largeau, C., 2004. Effects of hydrocarbon structure on fatty acid,
661 fatty alcohols and β-hydroxy acid composition in the hydrocarbon-degrading bacterium
662 *Marinobacter hydrocarbonoclasticus*. Lipids 39, 491–505.
663 Stein, R., Fahl, K., Müller, J., 2012. Proxy reconstruction of Arctic Ocean sea ice history:
664 from IRD to IP_{25}. Polarforschung 82 (1), 37–71.
665 Swaving, J., de Bont, A.M., 1998. Microbial transformation of epoxides. Enzyme and
666 Microbial Technology 22, 19–26.
667 Vare, L.L., Massé, G., Gregory, T.R., Smart, C.W., Belt, S.T., 2009. Sea ice variations in
668 the central Canadian Arctic Archipelago during the Holocene. Quaternary Science
669 Reviews 28, 1354–1366.
670 Volkman, J.K., Barrett, S.M., Dunstan, G.A., 1994. C_{25} and C_{30} highly branched isoprenoid
671 alkenes in laboratory cultures of two marine diatoms. Organic Geochemistry 21, 407–
672 414.
673 Xiao, X., Stein, R., Fahl, K., 2013. Biomarker distributions in surface sediments from the
674 Kara and Laptev Seas (Arctic Ocean): Indicators for organic-carbon sources and sea ice
675 coverage. Quaternary Science Reviews 79, 40–52.

676 Zabeti, N., Bonin, P., Volkman, J.K., Jameson, I., Guasco, S., Rontani, J.-F., 2010. Potential
677 alteration of $U_{37}^{K'}$ paleothermometer due to selective degradation of alkenones by marine
678 bacteria isolated from the haptophyte *Emiliania huxleyi*. FEMS Microbiology and
679 Ecology 73, 83–94.

APPENDIX

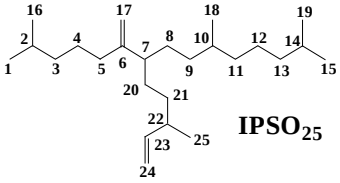

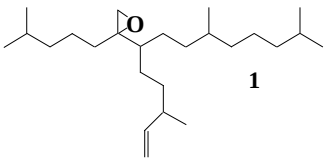
1

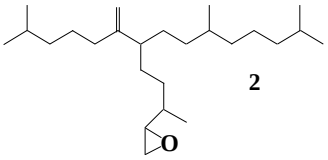
2

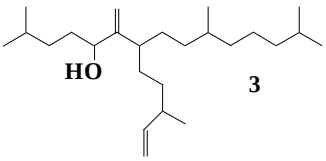
3

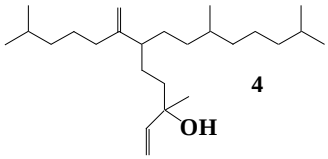
4

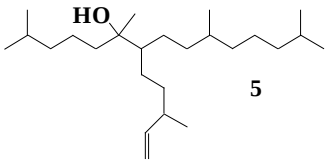
5

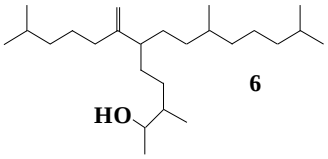
6

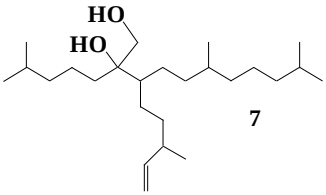
7

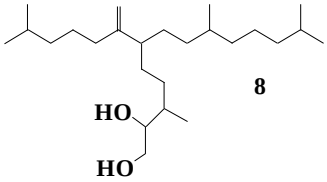
8

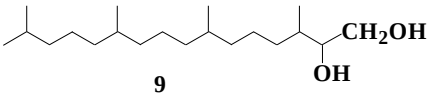
9

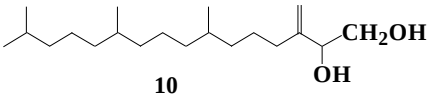
10

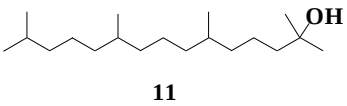
11

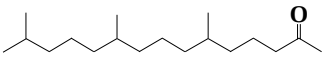
12

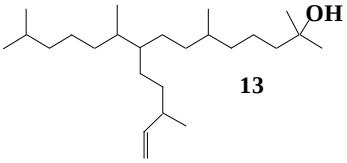
13

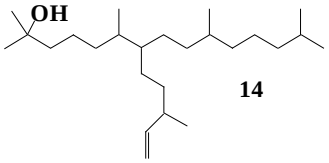
14

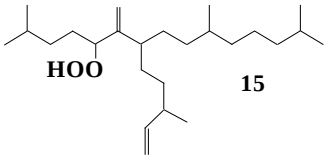
15

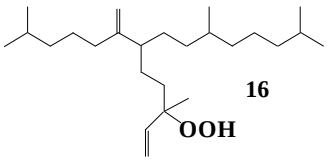
16

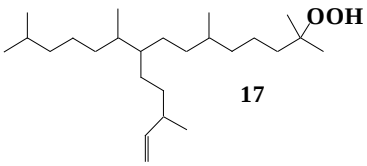
17

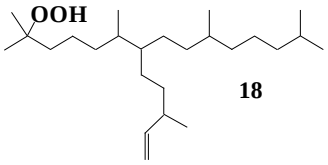
18

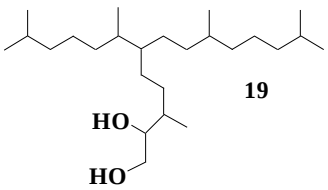
19

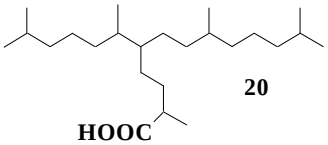
20

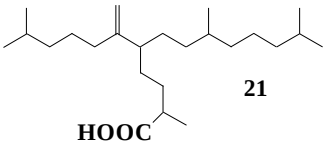
21

681 FIGURE CAPTIONS

682

683 **Figure 1**. TOFMS mass spectra of 1,2-epoxy-2-(4-methylpentyl)-3-(3-methylpent-4-enyl)-
684 6,10-dimethylundecane (**1**) (A) and trimethylsilyl derivatives of: 6-methylidene-2,10,14-
685 trimethyl-7-(3-methylpent-4-enyl)-pentadecan-5-ol (**3**) (B), 3,9,13-trimethyl-6-(1-
686 methylidene-5-methylhexyl)-tetradec-1-en-3-ol (**4**) (C) and 10-methylidene-2,6,14-
687 trimethyl-9-(3-methylpent-4-enyl)-pentadecan-2-ol (**13**) or 6-methylidene-2,10,14-
688 trimethyl-7-(3-methylpent-4-enyl)-pentadecan-2-ol (**14**) (D).

689

690 **Figure 2**. TOFMS mass spectra of trimethylsilyl derivatives of: 2,6,10,14-tetramethyl-7-(3-
691 methylpent-4-enyl)-pentadecan-6-ol (**5**) (A), 3,9,13-trimethyl-6-(1-methylidene-5-
692 methylhexyl)-tetradecan-2-ol (**6**) (B), 2-(4-methylpentyl)-3-(3-methylpent-4-enyl)-6,10-
693 dimethylundecane-1,2-diol (**7**) (C) and 3,9,13-trimethyl-6-(1-methylene-5-methylhexyl)-
694 tetradecane-1,2-diol (**8**) (D) .

695

696 **Figure 3**. MRM chromatograms (*m/z* 365 → 275, *m/z* 365 → 149 and *m/z* 425 → 135) of
697 silylated standard alcohol **3** (A) and DCM fractions obtained from the Antarctic station BC
698 313 (B) and the 10-11 cm sediment layer of the box core from Barrow Strait (Canadian
699 Arctic) (C).

700

701 **Figure 4**. MRM chromatograms (*m/z* 201 → 111, *m/z* 353 → 117, *m/z* 353 → 297 and *m/z*
702 423 → 367) of silylated standard alcohol **5** (A) and DCM fraction obtained from the 2-3 cm
703 sediment layer of the box core from Barrow Strait (Canadian Arctic) (B).

Figure 5. MRM chromatograms (*m/z* 526 → 231 and *m/z* 526 → 142) of silylated standard diol **7** (A) and DCM fractions obtained from the 2-3 cm (B) and the 10-11 cm (C) sediment layers of the box core from Barrow Strait (Canadian Arctic).

Figure 6. Proposed mechanisms for the autoxidation of $IPSO_{25}$ in sediments and subsequent $NaBH_4$-reduction of the resulting hydroperoxides during the treatment.

Figure 7. Proposed mechanisms for the formation and degradation of epoxides **1** and **2** in sediments.

Figure 8. Relative percentages of $IPSO_{25}$ and its degradation products in various sediment sections of the box core from Barrow Strait (Canadian Arctic).

Supplementary Figure 1. Antarctic (a) and Arctic (b) sampling locations. (The rectangle corresponds to the sampling zone of SPM, see Rontani et al., 2018b for more precise locations).

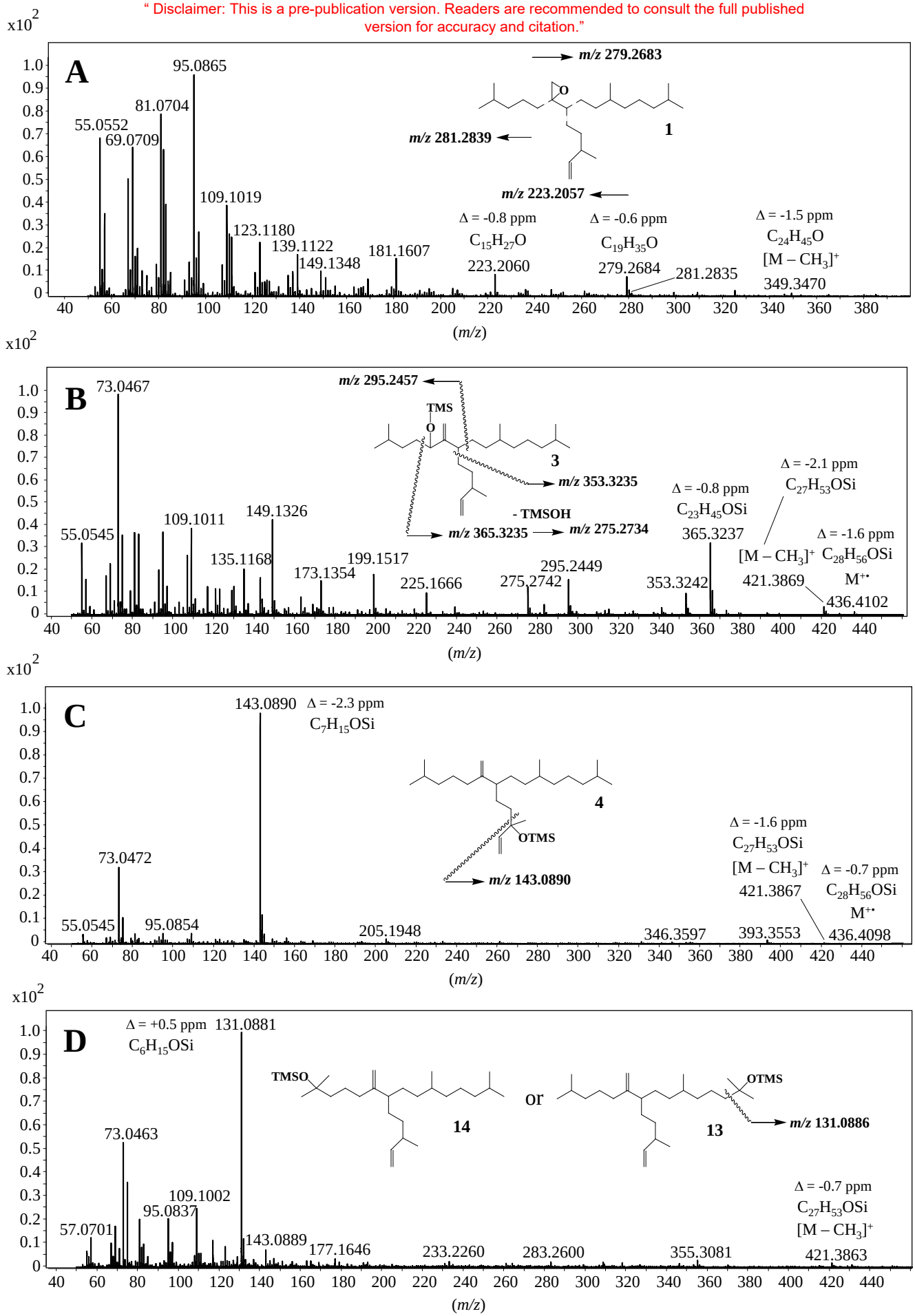

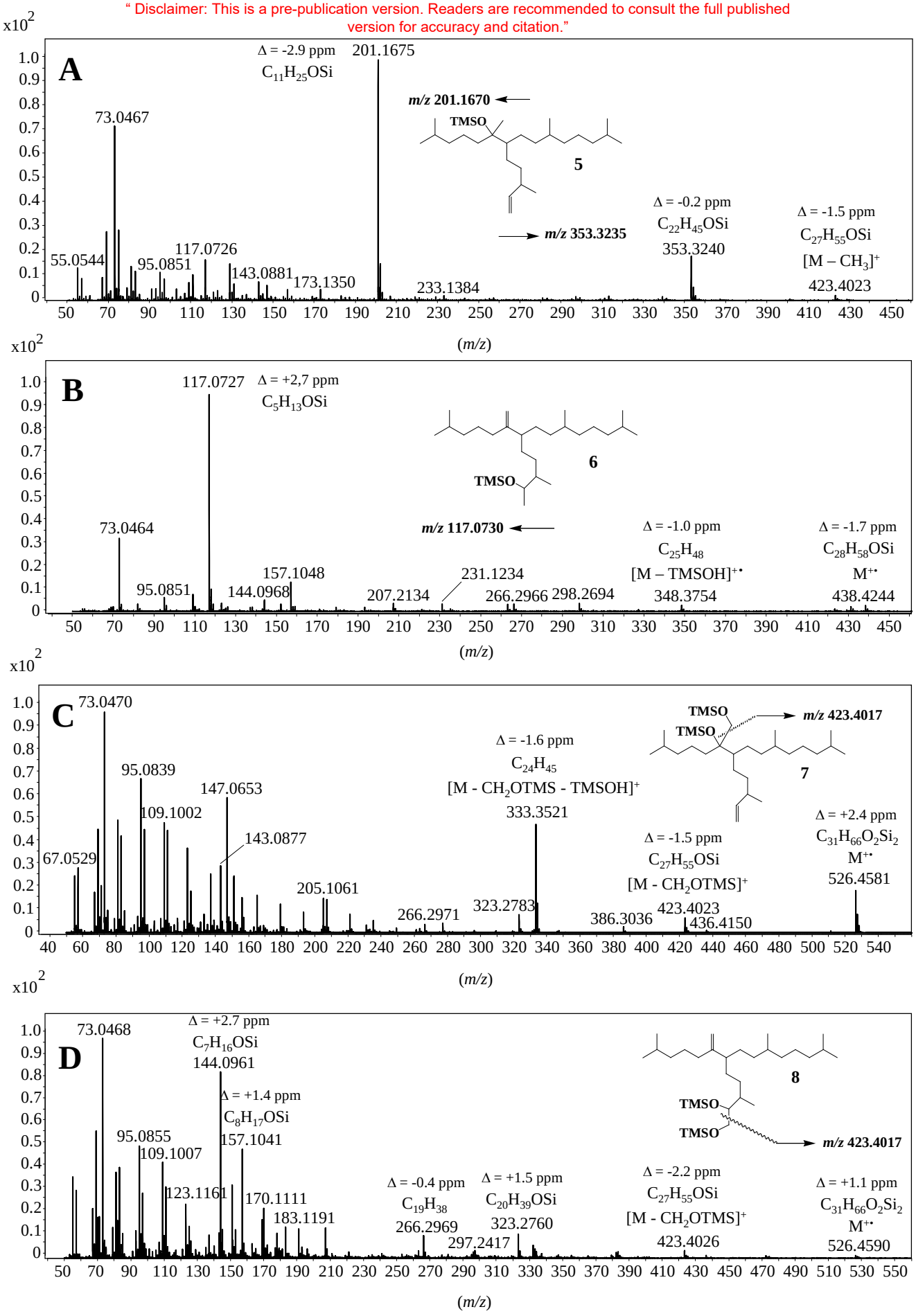

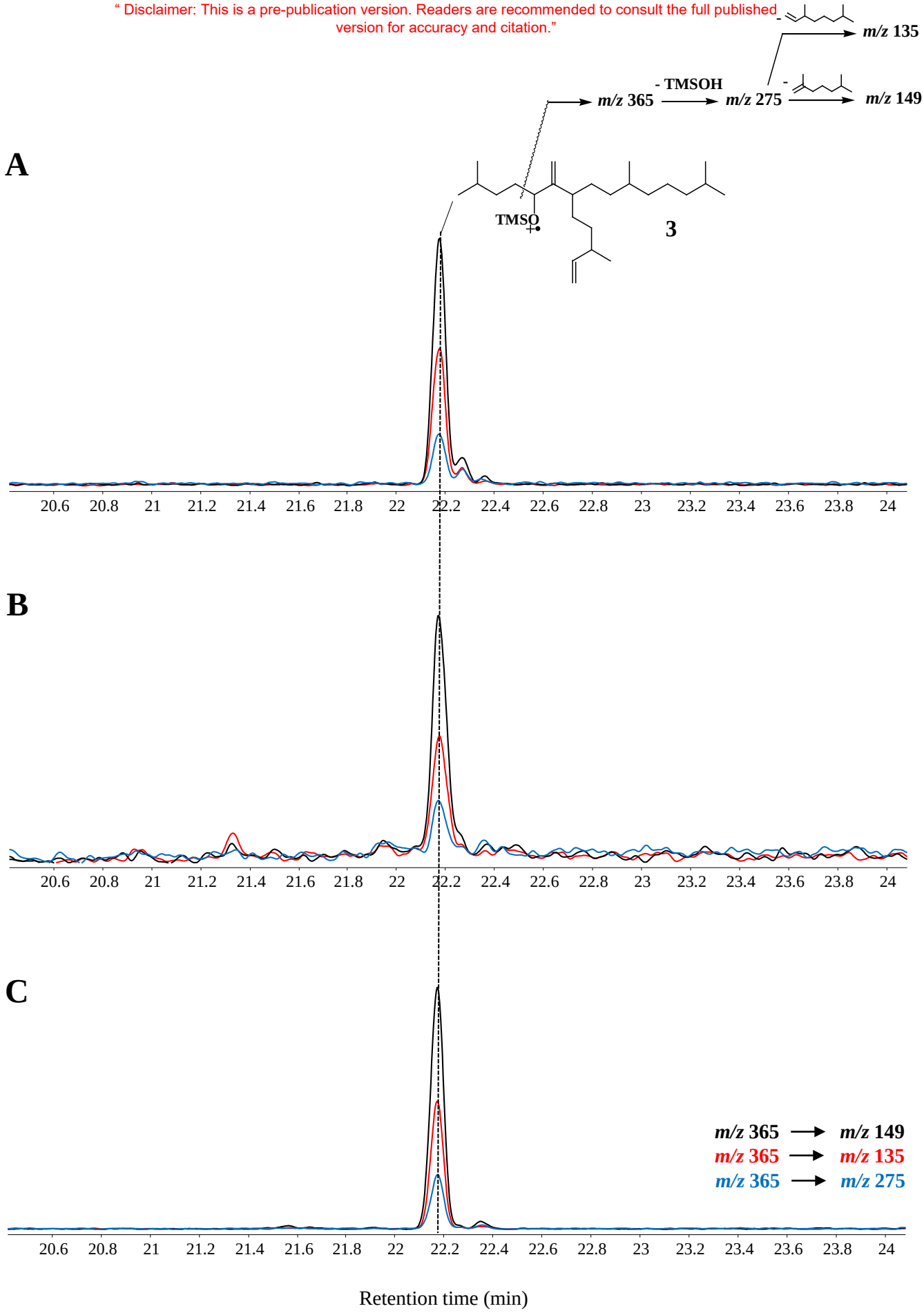

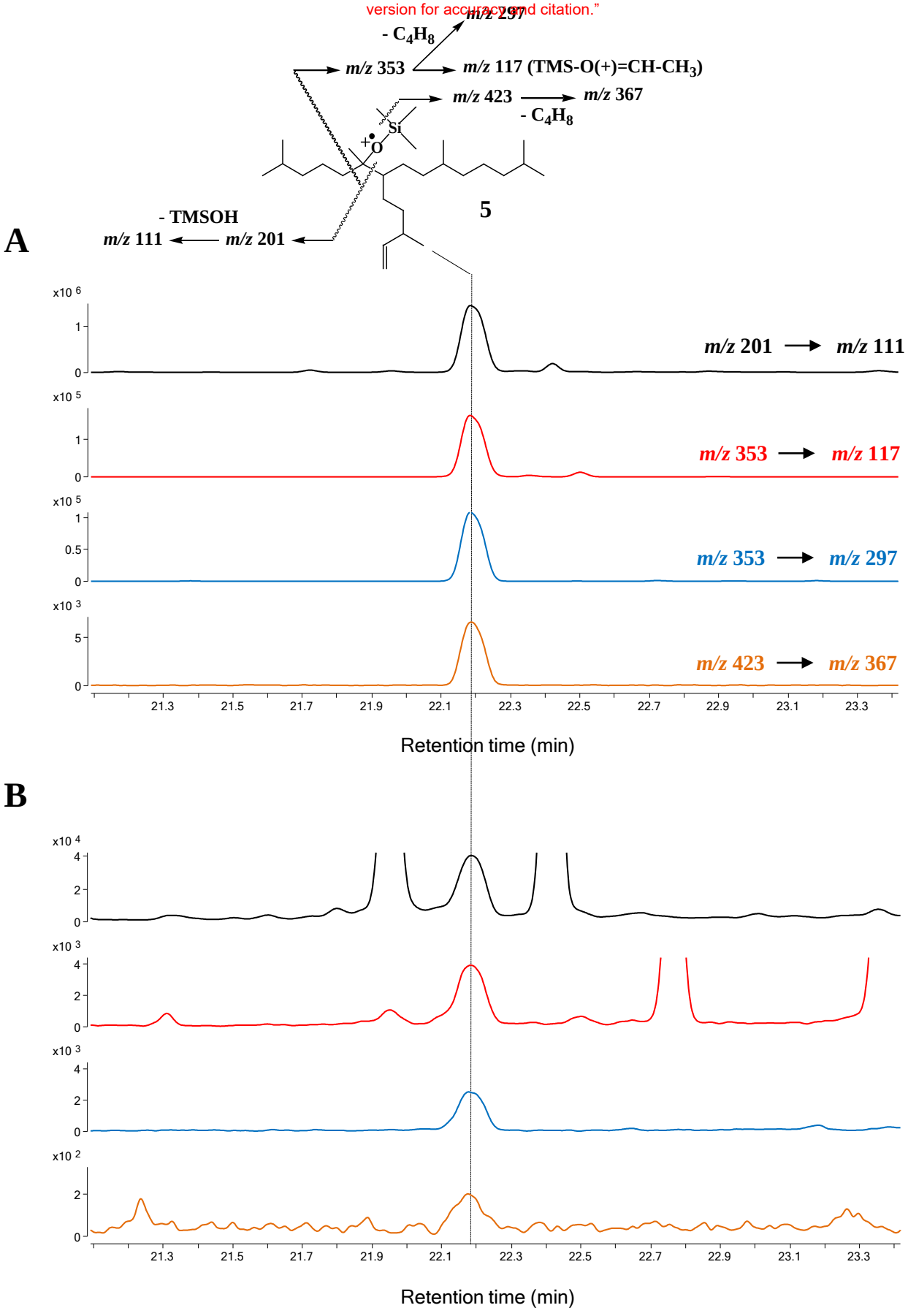

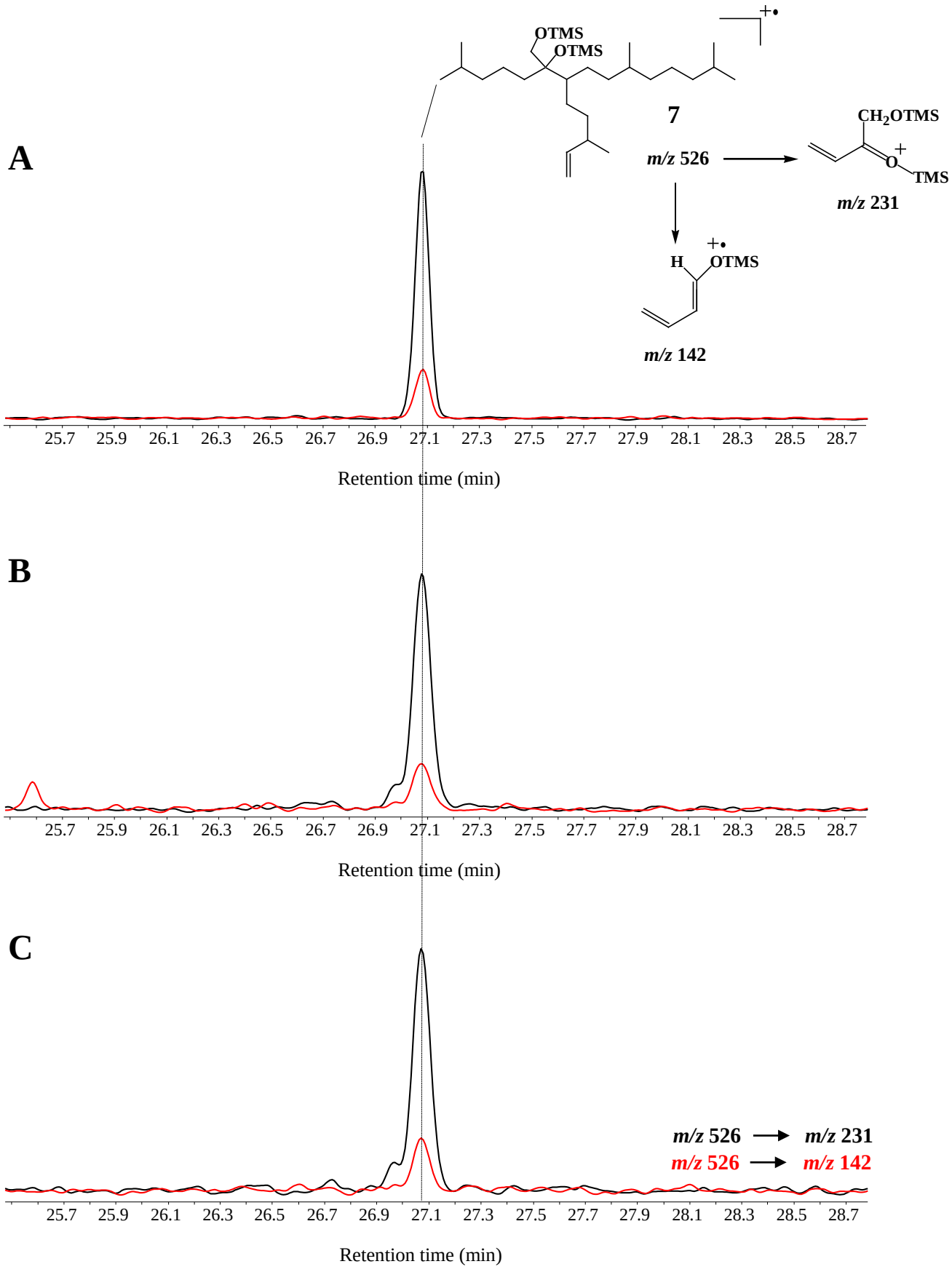

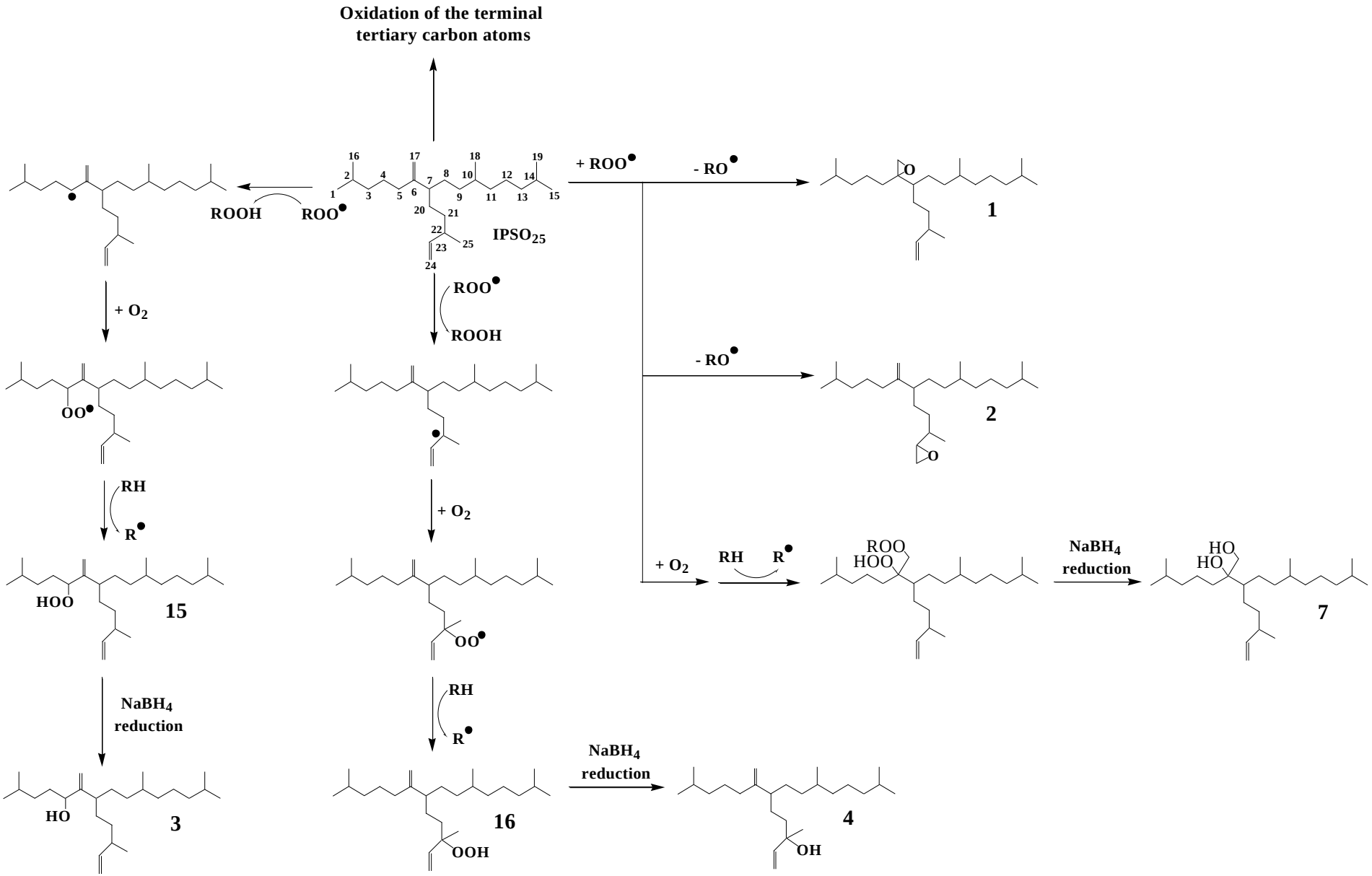

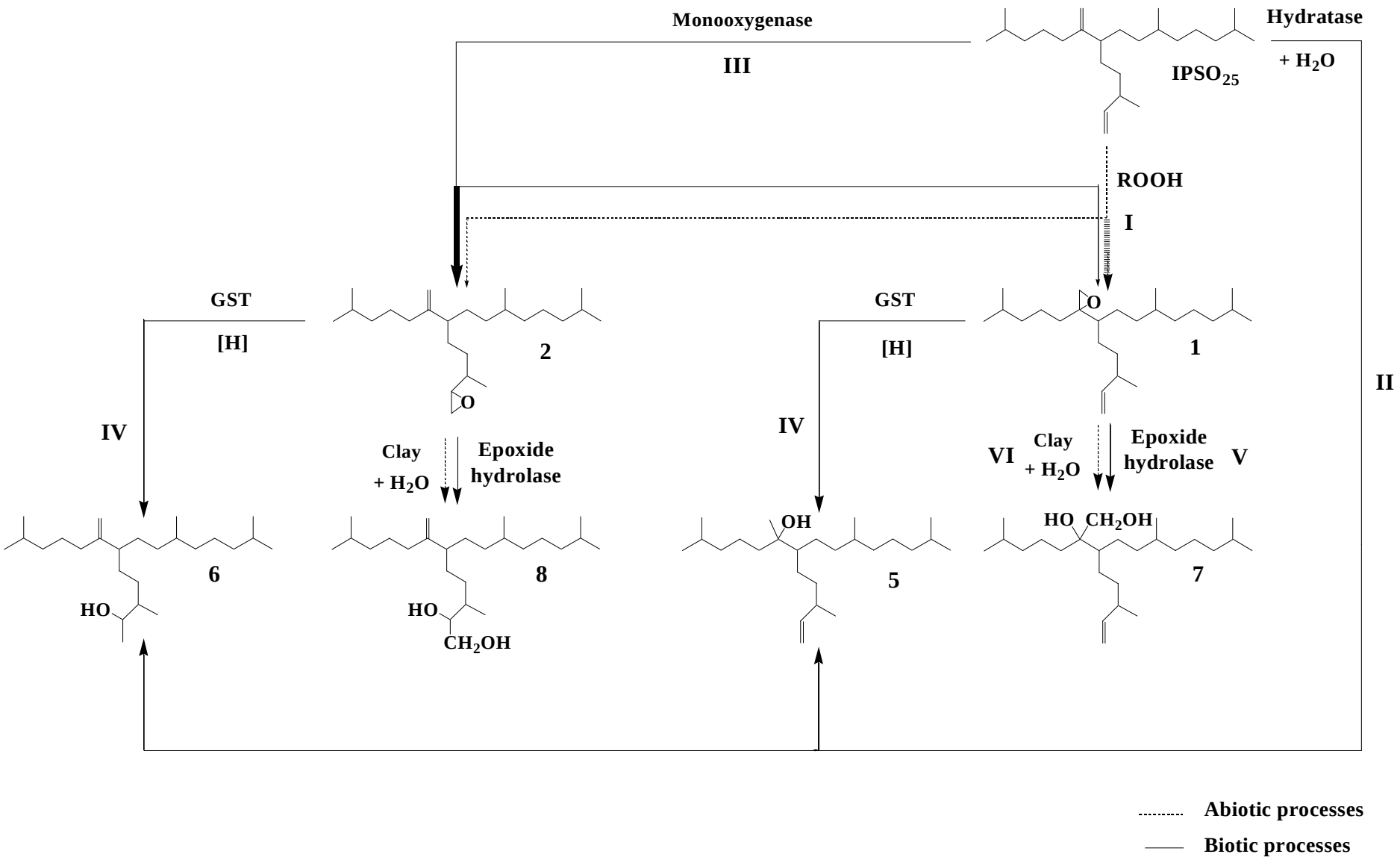

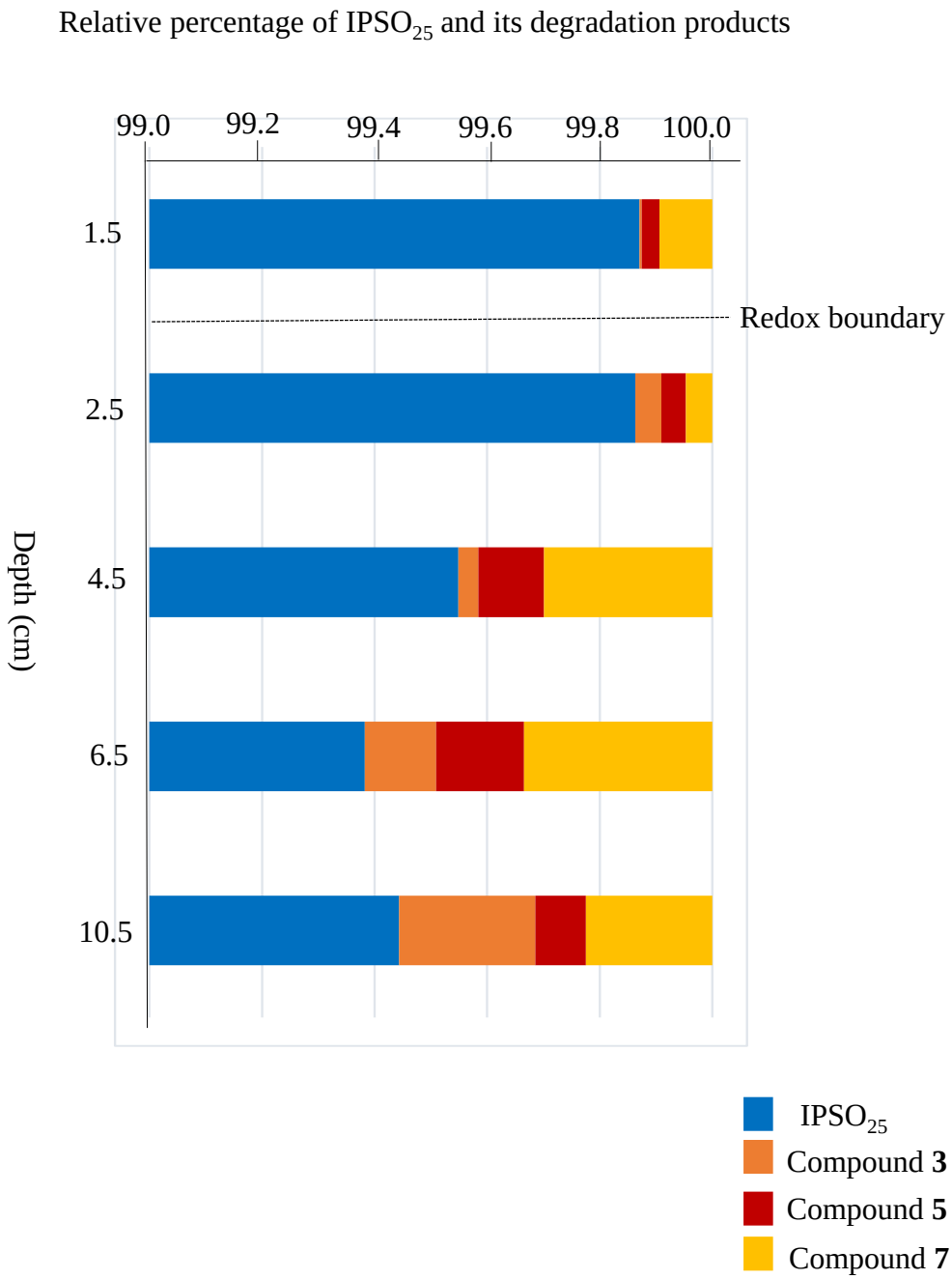

Table 1

Concentrations of $IPSO_{25}$ and its degradation products in Antarctic surface sediments

Station	$IPSO_{25}$ (ng g^{-1})	Compound **3** (pg g^{-1})	Compound **5** (pg g^{-1})
BC 313	1201.0	101.3 (0.01)[b]	77.8 (0.01)[b]
BC 316	396.0	569.2 (0.14)	38.1 (0.01)
BC 516	49.0	50.0 (0.10)	-
BC 566	42.0	230.3 (0.55)	231.7 (0.55)
BC 571	14.0	44.4 (0.32)	37.0 (0.26)
BC 615	93.0	-[a]	33.4 (0.04)
BC 628	29.0	54.5 (0.19)	25.4 (0.01)

[a] Not detected
[b] Percentage relative to the residual parent compound.

Table 2

Concentrations of $IPSO_{25}$ and its degradation products in sediments from the Arctic station 4 (Barrow Strait)

Depth (cm)	$IPSO_{25}$ ($\mu g\ g^{-1}$)	Compound **3** ($ng\ g^{-1}$)	Compound **5** ($ng\ g^{-1}$)	Compound **7** ($ng\ g^{-1}$)
1.5	2.5	0.1	0.8	2.4
2.5	3.2	1.5	1.4	1.5
4.5	2.0	0.7	2.3	5.9
6.5	1.7	2.2	2.7	5.8
8.5	1.6	0.2	0.1	0.6
10.5	1.8	4.3	1.6	4.0